Int. J. Heat Mass Transfer. Vol. 35, No. 1, pp. 207–220, 1992
Printed in Great Britain

0017-9310/92 $5.00+0.00

Non-parallel thermal instability of natural convection flow on non-isothermal inclined flat plates

H. R. LEE, T. S. CHEN and B. F. ARMALY
Department of Mechanical and Aerospace Engineering and Engineering Mechanics, University of Missouri–Rolla, Rolla, MO 65401, U.S.A.

(*Received* 19 *June* 1990 *and in final form* 24 *January* 1991)

Abstract—The vortex instability characteristics of laminar boundary-layer flow in natural convection on inclined flat plates heated from below, under the variable surface temperature $T_w(x)-T_\infty = Ax^n$, are studied analytically by the linear theory. The analysis is performed by using the non-parallel flow model in which the steady main flow is treated as two-dimensional and account is taken of the streamwise dependence of the disturbance amplitude functions. Neutral stability curves as well as critical Grashof numbers and the corresponding critical wave numbers are presented for fluids having $Pr = 0.7$ and 7 over the range of inclination angles, $0° \leqslant \phi \leqslant 70°$ from the horizontal, for a range of the exponent values n from $-1/3$ to 1. For a given Prandtl number and a given exponent value n, the flow is found to become more stable to the vortex mode of instability as the inclination angle increases from the horizontal. In addition, the local non-similarity non-parallel flow model provides a larger critical Grashof number than that of the local similarity non-parallel flow model. Results from the present non-parallel flow analysis are compared with previous results from the parallel flow analyses and with available experimental data. The streamwise dependence of the disturbances leads to a stabilization of the main flow, which brings the present predictions to a close and qualitative agreement with available experimental data.

INTRODUCTION

A FLOW pattern, laminar or transitional or turbulent, strongly affects the thermal transport process in convective heat transfer. For this reason, the study of flow instability or transition is of primary importance. Extensive experimental and analytical studies on the instability of natural convection flow over inclined, upward-facing heated surfaces have been performed (see, for example, refs. [1–15]). The instability of the flow that occurs as the result of a secondary flow in the form of longitudinal vortex rolls is due to the presence of a buoyancy force component that acts in the direction normal to the plate. From the experimental work of Lloyd and Sparrow [2] on natural convection flow in water over inclined heated plates, it was found that for inclination angles less than 14° from the vertical, the instability is characterized by the Tollmien–Schlichting wave mode, whereas the instability is characterized by the longitudinal vortex mode for inclination angles larger than 17° from the vertical. In the range between 14° and 17°, the two modes of instability were found to coexist in this zone of continuous transition. Their experimental finding has led to many analytical studies on the vortex instability for such a flow configuration.

In most of the analytical studies [3–6] on the vortex mode of instability of laminar flow over inclined heated plates, the main flow and thermal fields employed in the analyses were approximated by the similarity solution for a vertical flat plate; that is, the normal component of the buoyancy force that induces the streamwise pressure gradient in the main flow was neglected. This approximate analysis yielded considerable errors in the critical Grashof numbers when the angles of inclination from the horizontal are small, as was reported in a recent study by Chen and Tzuoo [10] who employed a new main flow solution for the non-similar boundary layer in their analysis. Their study is an improvement over the previous analyses, but as in the other earlier studies the streamwise dependence of the disturbances was not taken into account. Thus, in all of the analytical studies [3–6, 10, 11], a linear parallel flow model is employed, in which the amplitude functions of the disturbances are assumed to be independent of the streamwise coordinate. The parallel flow analysis has provided critical Grashof numbers that are two to three orders of magnitude lower than the experimental values. There is strong evidence from recent studies on the vortex instability of natural convection flow over a horizontal flat plate [15] and the vortex instability of forced convection flow [16–18] to indicate that the non-parallel flow analysis will yield more realistic predictions of the instability characteristics, when compared with experimental data, than the parallel flow analysis. This has motivated the present study.

In the present study, attention is focused on the vortex instability of natural convection flow over inclined, upward-facing heated plates by employing the non-parallel flow model in which account is taken of the streamwise variation of the disturbances. The surface temperature of the plate is treated as non-uniform and varies as $T_w(x)-T_\infty = Ax^n$. In the analysis, the disturbance quantities are properly scaled and

NOMENCLATURE

a dimensionless wave number of disturbance, $\alpha X^{-2/5}$
D partial derivative with respect to η
f reduced stream function, $\psi(x, y)/[5\nu(Gr_x \cos\phi/5)^{1/5}]$
g gravitational acceleration
Gr_x local Grashof number, $g\beta[T_w(x)-T_\infty]x^3/\nu^2$
Gr_L Grashof number based on L, $g\beta[T_w(L)-T_\infty]L^3/\nu^2$
k thermal conductivity
L characteristic length
n exponent in the power-law variation of the wall temperature
Nu_x local Nusselt number
p' disturbance pressure
P mainflow pressure
Pr Prandtl number
q_w local surface heat flux
t dimensionless amplitude function of temperature disturbance
t' disturbance temperature
T main flow temperature
u, v, w dimensionless amplitude functions of velocity disturbance in the x-, y-, z-directions, respectively
u', v', w' streamwise, normal, and spanwise components of disturbance velocity
U, V streamwise and normal velocity components of main flow in the x-, y-directions, respectively
x, y, z streamwise, normal, and spanwise coordinates
X, Y, Z dimensionless streamwise, normal, and spanwise coordinates, defined, respectively, as x/L, $y/(\varepsilon L)$, $z/(\varepsilon L)$.

Greek symbols
α dimensionless wave number of disturbances, $2\pi/\lambda$
β volumetric coefficient of thermal expansion
ε dimensionless parameter, $(Gr_L \cos\phi/5)^{-1/5}$
η pseudo-similarity variable, $(y/x)(Gr_x \cos\phi/5)^{1/5}$
θ dimensionless temperature, $(T-T_\infty)/[T_w(x)-T_\infty]$
κ thermal diffusivity of fluid
λ dimensionless wavelength
μ dynamic viscosity of fluid
ν kinematic viscosity of fluid
ξ non-similarity parameter, $(Gr_x \cos\phi/5)^{1/5} \tan\phi$
ρ density of fluid
σ function, $\partial u/\partial \xi$
τ function, $\partial t/\partial \xi$
τ_w local wall shear stress
ϕ angle of inclination from the horizontal
ψ stream function
ω function, $\partial v/\partial \xi$.

Superscripts
$+$ dimensionless disturbance quantity
$-$ scale quantity defined by equation (20)
$*$ critical condition or dimensionless main flow quantity
resultant quantity.

Subscripts
0 dimensionless amplitude function
w condition at the wall
∞ condition at the free stream.

the resulting partial differential equations for the disturbance amplitude functions, along with the boundary conditions, are converted into an eigenvalue problem by employing either the local similarity (three-equation) non-parallel flow model or the local non-similarity (six-equation) non-parallel flow model. The eigenvalue problem for each model is solved numerically by an efficient finite-difference method [19] in conjunction with Müller's shooting iteration technique.

Numerical results of interest, such as the neutral stability curves, critical Grashof numbers, and critical wave numbers are presented for fluids having Prandtl numbers of $Pr = 0.7$ and 7 over the inclination angles from the horizontal, $0° \leqslant \phi \leqslant 70°$, and a range of the exponent values, $-1/3 \leqslant n \leqslant 1$. The present results from the local similarity and the local non-similarity non-parallel flow models are compared with those from the previous studies based on the parallel flow model and with available experimental data.

ANALYSIS

The main flow and thermal fields

As the first step in the analysis of the vortex instability of the flow, attention is directed to the main flow and thermal fields. Consider an inclined flat plate which makes an acute angle ϕ from the horizontal, with its heated surface facing upward in an otherwise quiescent fluid at temperature T_∞. The physical coordinates are chosen such that x is measured from the leading edge of the plate and y is measured normal to the plate. The surface temperature of the plate varies as $T_w(x)-T_\infty = Ax^n$ where A and the exponent n are real constants. Under the assumption of constant fluid properties and using the Boussinesq approximation, the governing conservation equations for the main flow and thermal fluids can be written as [20]

$$f''' + (n+3)ff'' - (2n+1)(f')^2 + \xi\theta + \frac{1}{5}\left[(2-n)\eta\theta + (4n+2)\int_\eta^\infty \theta\,\mathrm{d}\eta + (n+3)\xi\int_\eta^\infty \frac{\partial\theta}{\partial\xi}\mathrm{d}\eta\right] = (n+3)\xi\left[f'\frac{\partial f'}{\partial\xi} - f''\frac{\partial f}{\partial\xi}\right] \quad (1)$$

$$\theta'' + (n+3)Pr\,f\theta' - 5n\,Pr\,f'\theta = (n+3)Pr\,\xi\left[f'\frac{\partial\theta}{\partial\xi} - \theta'\frac{\partial f}{\partial\xi}\right] \quad (2)$$

$$f'(\xi,0) = 0, \quad f(\xi,0) + \xi\,\partial f(\xi,0)/\partial\xi = 0,$$
$$f'(\xi,\infty) = 0, \quad \theta(\xi,0) = 1, \quad \theta(\xi,\infty) = 0 \quad (3)$$

where the pseudo-similarity variable $\eta(x, y)$, the non-similarity parameter $\xi(x)$, the dimensionless stream function $f(\xi, \eta)$, and the dimensionless temperature $\theta(\xi, \eta)$ are defined, respectively, as

$$\eta = (y/x)(Gr_x\cos\phi/5)^{1/5},$$
$$\xi(x) = (Gr_x\cos\phi/5)^{1/5}\tan\phi,$$
$$f(\xi,\eta) = \psi(x,y)/[5\nu(Gr_x\cos\phi/5)^{1/5}],$$
$$\theta(\xi,\eta) = (T-T_\infty)/[T_w(x)-T_\infty] \quad (4)$$

with $Gr_x = g\beta[T_w(x)-T_\infty]x^3/\nu^2$ denoting the local Grashof number and the angle ϕ being measured from the horizontal. The non-similar parameter $\xi(x)$ measures the combined effects of buoyancy force (Gr_x) and inclination angle (ϕ) on the flow and heat transfer characteristics. In equations (1)–(3) the primes stand for partial differentiations with respect to η and Pr is the Prandtl number. Other notations are as defined in the Nomenclature.

Equations (1)–(3) were solved by an efficient finite-difference method [19] in conjunction with the cubic spline interpolation scheme to provide the main flow quantities that are needed in the instability calculations and to provide other physical quantities, such as the local Nusselt number Nu_x, the local wall shear stress τ_w, and the axial velocity distribution u. In terms of the dimensionless variables, these quantities can be expressed, repectively, by

$$Nu_x(Gr_x\cos\phi/5)^{-1/5} = -\theta'(\xi,0),$$
$$\tau_w(x^2/5\mu\nu)(Gr_x\cos\phi/5)^{-3/5} = f''(\xi,0),$$
$$(ux/5\nu)(Gr_x\cos\phi/5)^{-2/5} = f'(\xi,\eta). \quad (5)$$

It is noted here that the case of uniform wall temperature (UWT) corresponds to $n = 0$.

Formulation of the stability problem

In the present study, the linear non-parallel flow stability theory is employed in the analysis. In experiments [1, 2] the vortex rolls have been found to be unchanging with time and periodic in the spanwise direction. Thus, the disturbance quantities for velocity components u', v', w', pressure p' and temperature t' are assumed to be a function of (x, y, z), independent of time. These disturbance quantities are superimposed on the steady, two-dimensional main flow quantities U, V, $W = 0$, P and T to obtain the following resultant quantities $\hat{U}$, $\hat{V}$, $\hat{W}$, $\hat{P}$, and $\hat{T}$:

$$\hat{U}(x,y,z) = U(x,y) + u'(x,y,z)$$
$$\hat{V}(x,y,z) = V(x,y) + v'(x,y,z)$$
$$\hat{W}(x,y,z) = w'(x,y,z)$$
$$\hat{P}(x,y,z) = P(x,y) + p'(x,y,z)$$
$$\hat{T}(x,y,z) = T(x,y) + t'(x,y,z). \quad (6)$$

Thus, the disturbance quantities are considered to be dependent on the streamwise coordinate x, in addition to the normal (y) and spanwise (z) coordinates. This is in contrast to most previous studies in which the disturbances are taken to be independent of x. The resultant quantities given by equation (6) satisfy the continuity equation, the Navier–Stokes equations, and the energy equation for an incompressible, three-dimensional steady fluid flow. Substituting equation (6) into these equations, subtracting the two-dimensional main flow, and linearizing the disturbance quantities, one can arrive at the following disturbance equations:

$$\frac{\partial u'}{\partial x} + \frac{\partial v'}{\partial y} + \frac{\partial w'}{\partial z} = 0 \quad (7)$$

$$u'\frac{\partial U}{\partial x} + U\frac{\partial u'}{\partial x} + v'\frac{\partial U}{\partial y} + V\frac{\partial u'}{\partial y} = -\frac{1}{\rho}\frac{\partial p'}{\partial x} + \nu\nabla^2 u' + g\beta\sin\phi t' \quad (8)$$

$$u'\frac{\partial V}{\partial x} + U\frac{\partial v'}{\partial x} + v'\frac{\partial V}{\partial y} + V\frac{\partial v'}{\partial y} = -\frac{1}{\rho}\frac{\partial p'}{\partial y} + \nu\nabla^2 v' + g\beta\cos\phi t' \quad (9)$$

$$U\frac{\partial w'}{\partial x} + V\frac{\partial w'}{\partial y} = -\frac{1}{\rho}\frac{\partial p'}{\partial z} + \nu\nabla^2 w' \quad (10)$$

$$u'\frac{\partial T}{\partial x} + U\frac{\partial t'}{\partial x} + v'\frac{\partial T}{\partial y} + V\frac{\partial t'}{\partial y} = \kappa\nabla^2 t' \quad (11)$$

where $\nabla^2 = \partial^2/\partial x^2 + \partial^2/\partial y^2 + \partial^2/\partial z^2$ is the Laplacian operator.

Since the disturbances are confined within the boundary layer of the main flow, the so-called bottling effect by Haaland and Sparrow [4], the disturbances will have length scales different from those of the main flow field [12, 13]. To verify this, the disturbance equations are first nondimensionalized by using the length and velocity scales of the main flow. The coordinates are scaled as

$$X = \frac{x}{L}, \quad Y = \frac{y}{\varepsilon L}, \quad Z = \frac{z}{\varepsilon L} \quad (12)$$

where $\varepsilon = (Gr_L\cos\phi/5)^{-1/5}$ and $Gr_L = g\beta[T_w(L)-T_\infty]L^3/\nu^2$ is the Grashof number based on the characteristic length $L(x)$. If $L = x$, then $Y = \eta$ and $Gr_L = Gr_x$. Other main flow quantities are scaled as

$$U^* = \frac{U\varepsilon^2 L}{\nu}, \quad V^* = \frac{V\varepsilon L}{\nu}, \quad \theta = \frac{T - T_\infty}{T_w(x) - T_\infty} \tag{13}$$

where U^*, V^*, and θ and their derivatives with respect to X and Y are of the order of 1. Similarly, the disturbance quantities can be scaled as

$$u^+ = \frac{u'\varepsilon^2 L}{\nu}, \quad v^+ = \frac{v'\varepsilon^2 L}{\nu}, \quad w^+ = \frac{w'\varepsilon^2 L}{\nu},$$

$$p^+ = \frac{p'\varepsilon^3 L^2}{\mu\nu}, \quad t^+ = \frac{t'}{T_w(x) - T_\infty} \tag{14}$$

where u^+, v^+, w^+, p^+, and t^+ and their derivatives with respect to X and Y are of the order of ε.

Substituting the above dimensionless variables from equations (12)–(14) into equations (7)–(11) one arrives at

$$\varepsilon\frac{\partial u^+}{\partial X} + \frac{\partial v^+}{\partial Y} + \frac{\partial w^+}{\partial Z} = 0 \tag{15}$$

$$u^+\frac{\partial U^*}{\partial X} + U^*\frac{\partial u^+}{\partial X} + \frac{v^+}{\varepsilon}\frac{\partial U^*}{\partial Y} + V^*\frac{\partial u^+}{\partial Y} = -\varepsilon\frac{\partial p^+}{\partial X} + \varepsilon^2\frac{\partial^2 u^+}{\partial X^2} + \frac{\partial^2 u^+}{\partial Y^2} + \frac{\partial^2 u^+}{\partial Z^2} + \frac{5}{\varepsilon}\tan\phi t^+ \tag{16}$$

$$\varepsilon u^+\frac{\partial V^*}{\partial X} + U^*\frac{\partial v^+}{\partial X} + v^+\frac{\partial V^*}{\partial Y} + V^*\frac{\partial v^+}{\partial Y} = -\frac{\partial p^+}{\partial Y} + \varepsilon^2\frac{\partial^2 v^+}{\partial X^2} + \frac{\partial^2 v^+}{\partial Y^2} + \frac{\partial^2 v^+}{\partial Z^2} + \frac{5}{\varepsilon}t^+ \tag{17}$$

$$U^*\frac{\partial w^+}{\partial X} + V^*\frac{\partial w^+}{\partial Y} = -\frac{\partial p^+}{\partial Z} + \varepsilon^2\frac{\partial^2 w^+}{\partial X^2} + \frac{\partial^2 w^+}{\partial Y^2} + \frac{\partial^2 w^+}{\partial Z^2} \tag{18}$$

$$u^+\frac{\partial \theta}{\partial X} + U^*\frac{\partial t^+}{\partial X} + \frac{v^+}{\varepsilon}\frac{\partial \theta}{\partial Y} + V^*\frac{\partial t^+}{\partial Y} = \frac{1}{Pr}\left[\varepsilon^2\frac{\partial^2 t^+}{\partial X^2} + \frac{\partial^2 t^+}{\partial Y^2} + \frac{\partial^2 t^+}{\partial Z^2}\right]. \tag{19}$$

The terms $(v^+/\varepsilon)\,\partial U^*/\partial Y$ and $(5/\varepsilon)\tan\phi t^+$ in equation (16), the term $5t^+/\varepsilon$ in equation (17), and the term $(v^+/\varepsilon)\,\partial\theta/\partial Y$ in equation (19) are larger than the other terms in the corresponding equations by at least an order of $(1/\varepsilon)$. This means that the (X, Y, Z) variables as defined in equation (12) are not the appropriate normalization scales for the disturbances. Therefore, by rescaling the coordinates for the disturbance quantities and the disturbance pressure with the form

$$(\bar{X}, \bar{Y}, \bar{Z}, \bar{p}^+) = (X, Y, Z, p^+)\varepsilon^{-1/2} \tag{20}$$

one has

$$\varepsilon\frac{\partial u^+}{\partial \bar{X}} + \frac{\partial v^+}{\partial \bar{Y}} + \frac{\partial w^+}{\partial \bar{Z}} = 0 \tag{21}$$

$$\varepsilon u^+\frac{\partial U^*}{\partial X} + \varepsilon^{1/2}U^*\frac{\partial u^+}{\partial \bar{X}} + v^+\frac{\partial U^*}{\partial Y} + \varepsilon^{1/2}V^*\frac{\partial u^+}{\partial \bar{Y}} = -\varepsilon^2\frac{\partial \bar{p}^+}{\partial \bar{X}} + \varepsilon^2\frac{\partial^2 u^+}{\partial \bar{X}^2} + \frac{\partial^2 u^+}{\partial \bar{Y}^2} + \frac{\partial^2 u^+}{\partial \bar{Z}^2} + 5\tan\phi t^+ \tag{22}$$

$$\varepsilon^2 u^+\frac{\partial V^*}{\partial X} + \varepsilon^{1/2}U^*\frac{\partial v^+}{\partial \bar{X}} + \varepsilon v^+\frac{\partial V^*}{\partial Y} + \varepsilon^{1/2}V^*\frac{\partial v^+}{\partial \bar{Y}} = -\varepsilon\frac{\partial \bar{p}^+}{\partial \bar{Y}} + \varepsilon^2\frac{\partial^2 v^+}{\partial \bar{X}^2} + \frac{\partial^2 v^+}{\partial \bar{Y}^2} + \frac{\partial^2 v^+}{\partial \bar{Z}^2} + 5t^+ \tag{23}$$

$$\varepsilon^{1/2}U^*\frac{\partial w^+}{\partial \bar{X}} + \varepsilon^{1/2}V^*\frac{\partial w^+}{\partial \bar{Y}} = -\varepsilon\frac{\partial \bar{p}^+}{\partial \bar{Z}} + \varepsilon^2\frac{\partial^2 w^+}{\partial \bar{X}^2} + \frac{\partial^2 w^+}{\partial \bar{Y}^2} + \frac{\partial^2 w^+}{\partial \bar{Z}^2} \tag{24}$$

$$\varepsilon u^+\frac{\partial \theta}{\partial X} + \varepsilon^{1/2}U^*\frac{\partial t^+}{\partial \bar{X}} + v^+\frac{\partial \theta}{\partial Y} + \varepsilon^{1/2}V^*\frac{\partial t^+}{\partial \bar{Y}} = \frac{1}{Pr}\left[\varepsilon^2\frac{\partial^2 t^+}{\partial \bar{X}^2} + \frac{\partial^2 t^+}{\partial \bar{Y}^2} + \frac{\partial^2 t^+}{\partial \bar{Z}^2}\right]. \tag{25}$$

Because the terms $\varepsilon\,\partial u^+/\partial\bar{X}$, $\varepsilon^2\partial\bar{p}^+/\partial\bar{X}$, $\varepsilon^2\partial^2u^+/\partial\bar{X}^2$, $\varepsilon^2\partial^2v^+/\partial\bar{X}^2$, $\varepsilon^2\partial^2w^+/\partial\bar{X}^2$, and $\varepsilon^2\partial^2t^+/\partial\bar{X}^2$ in equations (21)–(25) are smaller than the rest of the terms in their respective equations, they can be omitted. The omission of these lowest order terms in the disturbance equations is consistent with the level of approximation of the main flow. With the above-mentioned terms deleted and by making use of equation (20), the disturbance equations are reduced to

$$\frac{\partial v^+}{\partial Y} + \frac{\partial w^+}{\partial Z} = 0 \tag{26}$$

$$u^+\frac{\partial U^*}{\partial X} + U^*\frac{\partial u^+}{\partial X} + (Gr_L\cos\phi/5)^{1/5}v^+\frac{\partial U^*}{\partial Y} + V^*\frac{\partial u^+}{\partial Y} = \frac{\partial^2 u^+}{\partial Y^2} + \frac{\partial^2 u^+}{\partial Z^2} + 5(Gr_L\cos\phi/5)^{1/5}\tan\phi t^+ \tag{27}$$

$$(Gr_L\cos\phi/5)^{-1/5}u^+\frac{\partial V^*}{\partial X} + U^*\frac{\partial v^+}{\partial X} + v^+\frac{\partial V^*}{\partial Y} + V^*\frac{\partial v^+}{\partial Y} = -\frac{\partial p^+}{\partial Y} + \frac{\partial^2 v^+}{\partial Y^2} + \frac{\partial^2 v^+}{\partial Z^2} + 5(Gr_L\cos\phi/5)^{1/5}t^+ \tag{28}$$

$$U^*\frac{\partial w^+}{\partial X} + V^*\frac{\partial w^+}{\partial Y} = -\frac{\partial p^+}{\partial Z} + \frac{\partial^2 w^+}{\partial Y^2} + \frac{\partial^2 w^+}{\partial Z^2} \tag{29}$$

$$u^+\frac{\partial\theta}{\partial X}+U^*\frac{\partial t^+}{\partial X}+(Gr_L\cos\phi/5)^{1/5}v^+\frac{\partial\theta}{\partial Y}+V^*\frac{\partial t^+}{\partial Y}$$
$$=\frac{1}{Pr}\left[\frac{\partial^2 t^+}{\partial Y^2}+\frac{\partial^2 t^+}{\partial Z^2}\right]. \quad (30)$$

Next, the pressure terms in equations (28) and (29) are eliminated by cross differentiation and subtraction. The resulting equation is then differentiated with respect to Z once and the substitution $\partial w^+/\partial Z = -\partial v^+/\partial Y$ from the continuity equation is employed to remove the terms involving the function w^+ and its derivatives. This sequence of operations will yield three equations for the disturbance quantities u^+, v^+, and t^+. For the non-parallel flow model considered here, these quantities are expressed as

$$(u^+,v^+,t^+)=[u_0(X,Y),v_0(X,Y),t_0(X,Y)]\exp(\mathrm{i}a Z) \quad (31)$$

where a is the dimensionless azimuthal wave number of the disturbances. Thus, the longitudinal vortex rolls are taken to be periodic in the spanwise Z-direction, with the amplitude functions depending on both X and Y.

Substituting equation (31) into equation (27), the combined form of equations (28) and (29) as described above, and equation (30), along with introducing the coordinate transformation from (X, Y) to (X, η) through the relationship

$$Y=X^{2/5}\eta,\quad \frac{\partial}{\partial Y}=X^{-2/5}\frac{\partial}{\partial\eta},$$
$$Y\frac{\partial}{\partial Y}=Y\frac{\partial}{\partial\eta}\frac{\partial\eta}{\partial Y}=\eta\frac{\partial}{\partial\eta} \quad (32)$$

and letting

$$\alpha^2=a^2X^{4/5},\quad u=u_0,\quad v=v_0,\quad t=t_0X^{1/5} \quad (33)$$

one obtains the following system of partial differential equations for the disturbance amplitude functions u, v, and t:

$$\mathrm{D}^2u+\tilde a_1\mathrm{D}u+\tilde a_2u+\tilde a_3v+\tilde a_4t=5f'X\frac{\partial u}{\partial X} \quad (34)$$

$$\mathrm{D}^4v+\tilde b_1\mathrm{D}^3v+\tilde b_2\mathrm{D}^2v+\tilde b_3\mathrm{D}v+\tilde b_4v+\tilde b_5u+\tilde b_6t$$
$$=5f'X\frac{\partial}{\partial X}(\mathrm{D}^2v)+5f''X\frac{\partial}{\partial X}(\mathrm{D}v)-5\alpha^2f'X\frac{\partial v}{\partial X} \quad (35)$$

$$\mathrm{D}^2t+\tilde d_1\mathrm{D}t+\tilde d_2t+\tilde d_3u+\tilde d_4v=5Pr\,f'X\frac{\partial t}{\partial X}. \quad (36)$$

The corresponding boundary conditions are

$$u=v=\mathrm{D}v=t=0\quad \text{at }\eta=0\text{ and }\infty. \quad (37)$$

In equations (34)–(36) the coefficients $\tilde a_1,\ldots,\tilde a_4$, $\tilde b_1,\ldots,\tilde b_6$, and $\tilde d_1,\ldots,\tilde d_4$ are the mainflow quantities that are functions of (ξ, η). These coefficients will be defined later. Also, D^k stands for the kth partial derivative with respect to η. The boundary conditions (37) arise from the vanishing of the disturbances at the wall and in the free stream. The condition $\mathrm{D}v = 0$ results from the continuity equation (26) along with $w = 0$ at $\eta = 0$ and ∞.

Next, since the mainflow and thermal fields are expressed as functions of (ξ, η), it is convenient to express the disturbance amplitude functions u, v, and t also as functions of (ξ, η). From the $\xi(X)$ relationship, one has

$$X\frac{\partial}{\partial X}=X\frac{\partial}{\partial\xi}\frac{\mathrm{d}\xi}{\mathrm{d}X}+X\frac{\partial}{\partial\eta}\frac{\partial\eta}{\partial X}=\frac{3}{5}\xi\frac{\partial}{\partial\xi}-\frac{2}{5}\eta\frac{\partial}{\partial\eta}. \quad (38)$$

In terms of (ξ, η), equations (34)–(36) reduce to

$$\mathrm{D}^2u+a_1^*\mathrm{D}u+a_2^*u+a_3^*v+a_4^*t=3f'\xi\frac{\partial u}{\partial\xi} \quad (39)$$

$$\mathrm{D}^4v+b_1^*\mathrm{D}^3v+b_2^*\mathrm{D}^2v+b_3^*\mathrm{D}v+b_4^*v+b_5^*u+b_6^*t$$
$$=3f'\xi\frac{\partial}{\partial\xi}(\mathrm{D}^2v)+3f''\xi\frac{\partial}{\partial\xi}(\mathrm{D}v)-3\alpha^2f'\xi\frac{\partial v}{\partial\xi} \quad (40)$$

$$\mathrm{D}^2t+d_1^*\mathrm{D}t+d_2^*t+d_3^*u+d_4^*v=3Pr\,f'\xi\frac{\partial t}{\partial\xi} \quad (41)$$

along with boundary conditions given by equation (37). The coefficients in equations (39)–(41) are defined by

$$a_1^*=3f+3\xi\,\partial f/\partial\xi,$$
$$a_2^*=2\eta f''-f'-\alpha^2-3\xi\,\partial f'/\partial\xi,$$
$$a_3^*=-5f''(Gr_x\cos\phi/5)^{1/5},\quad a_4^*=5\xi,$$
$$b_1^*=3f+3\xi\,\partial f/\partial\xi,\quad b_2^*=5f'-2\alpha^2+3\xi\,\partial f'/\partial\xi,$$
$$b_3^*=2f''-3\alpha^2(f+\xi\,\partial f/\partial\xi),$$
$$b_4^*=\alpha^4+\alpha^2(2\eta f''-f'-3\xi\,\partial f'/\partial\xi),$$
$$b_5^*=(\alpha^2/5)(Gr_x\cos\phi/5)^{-1/5}(6f-2\eta f'$$
$$-4\eta^2f''+12\eta\xi\,\partial f'/\partial\xi-12\xi\,\partial f/\partial\xi-9\xi^2\,\partial^2f/\partial\xi^2),$$
$$b_6^*=-5\alpha^2(Gr_x\cos\phi/5)^{1/5},$$
$$d_1^*=3Pr(f+\xi\,\partial f/\partial\xi),\quad d_2^*=Pr\,f'-\alpha^2,$$
$$d_3^*=(Pr/5)(2\eta\theta'-3\xi\,\partial\theta/\partial\xi),$$
$$d_4^*=-Pr\,\theta'(Gr_x\cos\phi/5)^{1/5}. \quad (42)$$

Equations (39)–(41), along with boundary conditions (37), represent the mathematical system for the stability problem. Since equations (39)–(41) are partial differential equations, the boundary conditions as given by equation (37) are not sufficient if the ξ derivatives of u, v, and t are not set equal to zero. Two of the simple methods that can be used to solve such a system of equations are the local similarity and the local non-similarity methods [21, 22]. It is noted that when the terms on the right-hand side of equations (39)–(41) are deleted, the resulting equations along with boundary conditions (37) provide a system of three equations for the local similarity non-parallel flow model (the three-equation model). To obtain a system of equations for the local non-similarity non-parallel flow model, one first introduces

$$\sigma = \frac{\partial u}{\partial \xi}, \quad \omega = \frac{\partial v}{\partial \xi}, \quad \tau = \frac{\partial t}{\partial \xi}. \tag{43}$$

Equations (39)–(41) and (37) are then differentiated with respect to ξ once to obtain equations for σ, ω, and τ. If the terms involving $\partial\sigma/\partial\xi$, $\partial\omega/\partial\xi$, and $\partial\tau/\partial\xi$ in these equations are neglected (i.e. truncated), one can arrive at the following system of homogeneous 'ordinary differential equations' for the disturbance amplitude functions u, v, t, σ, ω, and τ:

$$D^2u + a_1Du + a_2u + a_3v + a_4t + a_5\sigma = 0 \tag{44}$$

$$D^4v + b_1D^3v + b_2D^2v + b_3Dv + b_4v + b_5u + b_6t + b_7D^2\omega + b_8D\omega + b_9\omega = 0 \tag{45}$$

$$D^2t + d_1Dt + d_2t + d_3u + d_4v + d_5\tau = 0 \tag{46}$$

$$D^2\sigma + e_1D\sigma + e_2\sigma + e_3\omega + e_4\tau + e_5Du + e_6u + e_7v + e_8t = 0 \tag{47}$$

$$D^4\omega + f_1D^3\omega + f_2D^2\omega + f_3D\omega + f_4\omega + f_5\sigma + f_6\tau + f_7D^3v + f_8D^2v + f_9Dv + f_{10}v + f_{11}u + f_{12}t = 0 \tag{48}$$

$$D^2\tau + g_1D\tau + g_2\tau + g_3\sigma + g_4\omega + g_5Dt + g_6t + g_7u + g_8v = 0 \tag{49}$$

with the boundary conditions

$$u = v = Dv = t = \sigma = \omega = D\omega = \tau = 0 \quad \text{at } \eta = 0 \text{ and } \infty. \tag{50}$$

The coefficients in equations (44)–(49) are defined in the Appendix.

The system of coupled differential equations (44)–(49), along with the homogeneous boundary conditions (50), now constitutes an eigenvalue problem of the form

$$E(\alpha, Gr_x; \phi, Pr, n) = 0. \tag{51}$$

This is the local non-similarity non-parallel flow model (the six-equation model).

For given values of the exponent n, Prandtl number Pr, and inclination angle ϕ, the value of wave number α satisfying equation (51) is sought as the eigenvalue for a prescribed value of the Grashof number Gr_x or the non-similarity parameter $\xi = (Gr_x \cos\phi/5)^{1/5}\tan\phi$.

NUMERICAL METHOD OF SOLUTIONS

The system of equations for the main flow and thermal fields, equations (1)–(3), was solved by a finite difference scheme in conjunction with a cubic spline interpolation procedure similar to, but modified from that described in ref. [19] to provide the main flow quantities $f, f', f'', \theta, \theta'$, and their partial derivatives with respect to ξ that are needed in the stability computations and in the determination of the local Nusselt number and the local wall shear stress. The stability problem, either consisting of equations (39)–(41) with their terms on the right-hand side deleted and equation (37), the three-equation local similarity non-parallel flow model, or consisting of equations (44)–(50) for the six-equation local non-similarity non-parallel flow model, was solved by a finite difference scheme along with Müller's shooting method. The solution method parallels that described in ref. [19] and, to conserve space, is not repeated here.

To proceed with the numerical calculations of the stability problem, the boundary conditions at $\eta = \eta_\infty$ need to be approximated by the asymptotic solutions of equations (39)–(41) with their terms on the right-hand side deleted, the three-equation model, or of equations (44)–(49) for the six-equation model at $\eta = \eta_\infty$ (i.e. at the edge of the boundary layer). In the six-equation model, since the mainflow quantities f', f'', θ, θ', and their ξ derivatives are zero at $\eta = \eta_\infty$, the asymptotic solutions for u, v, t, σ, ω, and τ at $\eta = \eta_\infty$ can be obtained as

$$\begin{gathered}
u_2 = \exp(-m\eta_\infty), \quad u_3 = \exp(-r\eta_\infty), \quad u_1 = u_4 = 0, \\
v_1 = \exp(-\alpha\eta_\infty), \quad v_2 = \exp(-m\eta_\infty), \\
v_3 = \exp(-r\eta_\infty), \quad v_4 = \eta_\infty\exp(-m\eta_\infty), \\
t_3 = \exp(-r\eta_\infty), \quad t_1 = t_2 = t_4 = 0, \\
\sigma_2 = \exp(-m\eta_\infty), \quad \sigma_3 = \exp(-r\eta_\infty), \quad \sigma_1 = \sigma_4 = 0, \\
\omega_1 = 0, \quad \omega_2 = \exp(-m\eta_\infty), \\
\omega_3 = \exp(-r\eta_\infty), \quad \omega_4 = \eta_\infty\exp(-m\eta_\infty), \\
\tau_3 = \exp(-r\eta_\infty), \quad \tau_1 = \tau_2 = \tau_4 = 0
\end{gathered} \tag{52}$$

where

$$\begin{aligned}
r &= \{-Pr\,C + [(Pr\,C)^2 + 4\alpha^2]^{1/2}\}/2 \\
m &= \{-C + [C^2 + 4\alpha^2]^{1/2}\}/2
\end{aligned} \tag{53}$$

with $C = -3f(\xi, \eta_\infty)$.

At any η location, the solutions for u, v, t, σ, ω, and τ are written as

$$\begin{aligned}
u(\xi,\eta) &= K_1u_1(\xi,\eta) + K_2u_2(\xi,\eta) + K_3u_3(\xi,\eta) + K_4u_4(\xi,\eta) \\
v(\xi,\eta) &= K_1v_1(\xi,\eta) + K_2v_2(\xi,\eta) + K_3v_3(\xi,\eta) + K_4v_4(\xi,\eta) \\
t(\xi,\eta) &= K_1t_1(\xi,\eta) + K_2t_2(\xi,\eta) + K_3t_3(\xi,\eta) + K_4t_4(\xi,\eta) \\
\sigma(\xi,\eta) &= K_1\sigma_1(\xi,\eta) + K_2\sigma_2(\xi,\eta) + K_3\sigma_3(\xi,\eta) + K_4\sigma_4(\xi,\eta) \\
\omega(\xi,\eta) &= K_1\omega_1(\xi,\eta) + K_2\omega_2(\xi,\eta) + K_3\omega_3(\xi,\eta) + K_4\omega_4(\xi,\eta) \\
\tau(\xi,\eta) &= K_1\tau_1(\xi,\eta) + K_2\tau_2(\xi,\eta) + K_3\tau_3(\xi,\eta) + K_4\tau_4(\xi,\eta)
\end{aligned} \tag{54}$$

where K_1, K_2, K_3, and K_4 are constants. In the three-equation local similarity model, the asymptotic solutions for u, v, and t at $\eta = \eta_\infty$ can be obtained in the same manner as shown in equations (52).

The stability problem is solved as follows. With a preassigned value of n, the main flow solution is first obtained for a given Prandtl number Pr and a fixed non-similarity parameter $\xi = (Gr_x \cos\phi/5)^{1/5} \tan\phi$. Next, with the angle ϕ selected, the Grashof number $Gr_x = (5/\cos\phi)(\xi/\tan\phi)^5$ is specified. With this known value of Gr_x and a guessed value of the wave number α as the eigenvalue, the finite difference form of equations (39)–(41) with their terms on the right-hand side deleted, the three-equation model, or the finite difference form of equations (44)–(49) for the six-equation model is numerically solved from $\eta = 0$ to η_∞, ending with the asymptotic solutions for u, v, t at $\eta = \eta_\infty$ for the three-equation model or for u, v, t, σ, ω, and τ at $\eta = \eta_\infty$ for the six-equation model. The guessed eigenvalue α is then corrected by Müller's shooting method until the boundary conditions at the wall ($\eta = 0$) are satisfied within a certain specified tolerance. This yields a converged α value as the eigenvalue for the given values of n, Pr, ϕ, and Gr_x.

After some experiments with the numerical solutions for the three-equation model, a step size of $\Delta\eta = 0.01$ and a value of $\eta_\infty = 10$ were found to provide accurate numerical results for both the main flow and stability calculations for all inclination angles ϕ. As for the numerical solutions of the six-equation model, a step size of $\Delta\eta = 0.01$ and a value of $\eta_\infty = 10$ were also found to be sufficient for all inclination angles ϕ larger than 10° for $Pr = 7$ and 15° for $Pr = 0.7$. However, for smaller angles of inclination, a smaller step size $\Delta\eta$ is needed to provide accurate stability results, although a step size of $\Delta\eta = 0.01$ and a value of $\eta_\infty = 10$ were sufficient to provide accurate numerical results for the main flow. This was verified by using a supercomputer with a larger memory capacity.

RESULTS AND DISCUSSION

To determine the stability and instability domains and to obtain the critical values of Grashof number (i.e. the minimum Grashof numbers for the incipiency of the vortex instability), neutral stability curves (i.e. the Grashof number vs wave number curves) were obtained. Numerical computations were first performed for the three-equation non-parallel flow model. The neutral stability curves for angles of inclination ϕ ranging from 0° to 70° from the horizontal with $n = 0$ (the uniform wall temperature, UWT, case) are plotted in Fig. 1 for fluids having Prandtl number of $Pr = 0.7$ and 7 which are typical for air and water, respectively. The results for $\phi = 0°$ (i.e. the horizontal flat plate) are taken from ref. [15]. It can be seen from Fig. 1 that for a given Prandtl number, the neutral stability curve shifts right-upward with increasing angle of inclination from the horizontal, ϕ. That is, the flow becomes more stable to the vortex

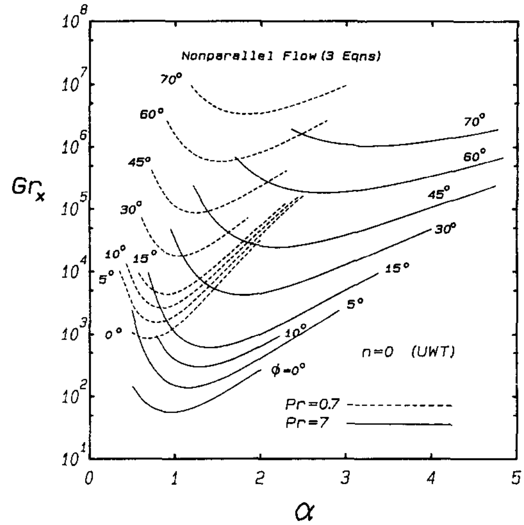

FIG. 1. The neutral stability curves from the three-equation non-parallel flow model, uniform wall temperature (UWT, $n = 0$), $Pr = 0.7$ and 7.

mode of instability as the angle of inclination increases from the horizontal toward the vertical orientation. For a vertical flat plate, the critical Grashof number from the vortex mode of instability becomes infinity. This is to be expected, because at the vertical orientation there is no buoyancy force component normal to the plate and hence the vortex instability of the flow does not take place.

For the three-equation non-parallel flow model, the critical values of the non-similarity parameter $\xi = (Gr_x \cos\phi/5)^{1/5} \tan\phi$ (denoted by ξ^*), the critical Grashof numbers Gr_x^*, and the corresponding critical wave numbers α^* from the present calculations are listed in Table 1 for the $n = 0$ (UWT) case.

The neutral stability curves from the six-equation non-parallel flow model for the case of $n = 0$ (UWT) are plotted in Fig. 2 for different inclination angles, ϕ. The results for $\phi = 0°$ (i.e. the horizontal flat plate) are also from ref. [15] since the six-equation model reduces to the three-equation model when $\xi = 0$ (i.e. $\phi = 0°$). It is noted here that to save the computation time and cost for the six-equation model, neutral stability curves were not obtained for inclination angles $\phi < 15°$ for $Pr = 0.7$ and for $\phi < 10°$ for $Pr = 7$. This was because a smaller step size, $\Delta\eta < 0.01$ (i.e. a larger storage space for computations), was needed to obtain accurate results for the small angles of inclination. To cope with the numerical difficulties associated with this, however, one can employ an interpolation method to obtain the results between the small angles of inclination and $\phi = 0°$, because accurate numerical results for $\phi = 0°$ are available in ref. [15]. This can be seen and expected from figures of critical Grashof number vs angle of inclination, to be presented later.

To compare the results between the six-equation and the three-equation non-parallel flow models, representative neutral stability curves for different

Table 1. Critical values of non-similar parameter, Grashof number, and wave number; three-equation local similarity non-parallel flow model; uniform wall temperature (UWT, $n = 0$)

ϕ (deg)	$Pr = 0.7$ ξ^*	Gr_x^*	α^*	$Pr = 7$ ξ^*	Gr_x^*	α^*
0	0	834.5	0.68803	0	56.3	0.94275
5	0.27524	1547	0.77197	0.16931	136.2	1.1402
10	0.61494	2619	0.83395	0.39624	290.9	1.2815
15	1.0271	4284	0.88765	0.69138	592.0	1.4068
30	2.8802	17 838	1.0437	2.1448	4085	1.7839
45	6.5671	86 368	1.2442	5.0923	24 213	2.2486
60	15.547	582 680	1.5273	12.247	176 744	2.7247
70	32.387	3 327 371	1.8299	25.571	1 020 907	3.2059

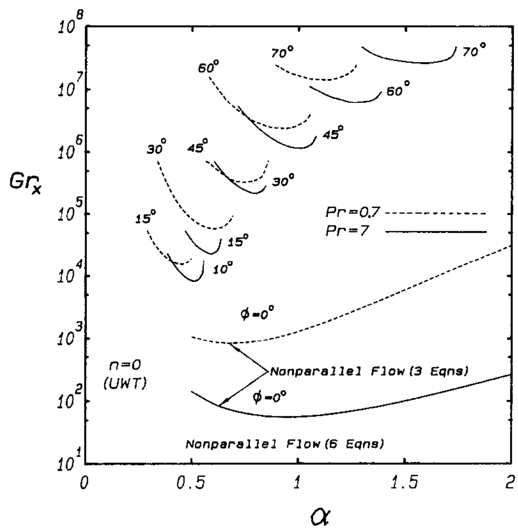

FIG. 2. The neutral stability curves from the six-equation non-parallel flow model, uniform wall temperature (UWT, $n = 0$), $Pr = 0.7$ and 7.

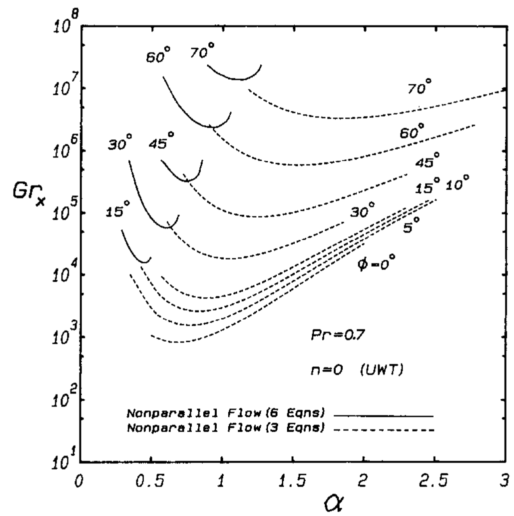

FIG. 3. A comparison of the neutral stability curves between the three-equation and the six-equation non-parallel flow models, uniform wall temperature (UWT, $n = 0$), $Pr = 0.7$.

inclination angles for the $n = 0$ (UWT) case are shown in Fig. 3 for $Pr = 0.7$ and in Fig. 4 for $Pr = 7$. One can see from these two figures that the six-equation non-parallel flow model gives rise to a larger critical Grashof number than that of the three-equation model, but at a smaller critical wave number. The neutral stability curves for the various n values, $n = -1/3$, 0 (UWT), 1/3, and 1 are compared in Figs. 5 and 6 for $Pr = 0.7$ and 7, respectively. In addition, the critical values of the non-similarity parameter $\xi = (Gr_x \cos\phi/5)^{1/5} \tan\phi$ (denoted by ξ^*), Grashof number Gr_x^*, and its wave number α^* are listed in Tables 2 and 3 for $n = -1/3$, 0 (UWT), 1/3, and 1. From Table 3, one can see that for $Pr = 7$, the critical Grashof number increases with increasing value of the exponent n for a given inclination angle $\phi < 60°$. However, for Prandtl number $Pr = 0.7$ (see Table 2), the critical Grashof number decreases with increasing value of the exponent n for angles ϕ that are large. All of these trends can also be seen in Fig. 7 for $Pr = 0.7$ and in Fig. 8 for $Pr = 7$.

Figures 9 and 10 show the critical Grashof numbers from the present analysis based on the three- and six-equation non-parallel flow models for $Pr = 0.7$ and

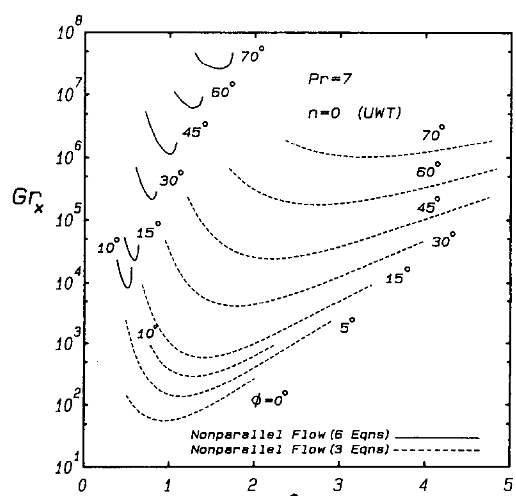

FIG. 4. A comparison of the neutral stability curves between the three-equation and the six-equation non-parallel flow models, uniform wall temperature (UWT, $n = 0$), $Pr = 7$.

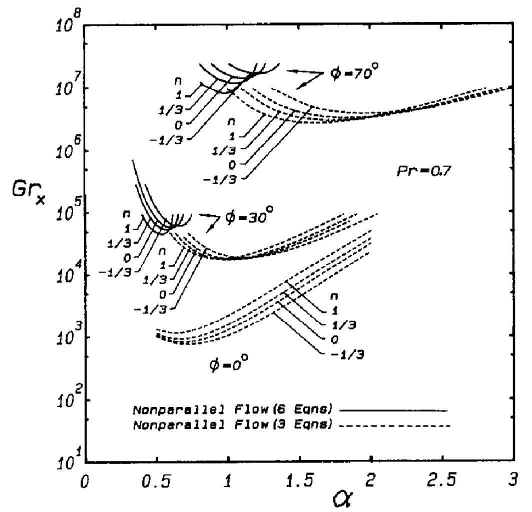

FIG. 5. The effect of n on the neutral stability curves, $Pr = 0.7$.

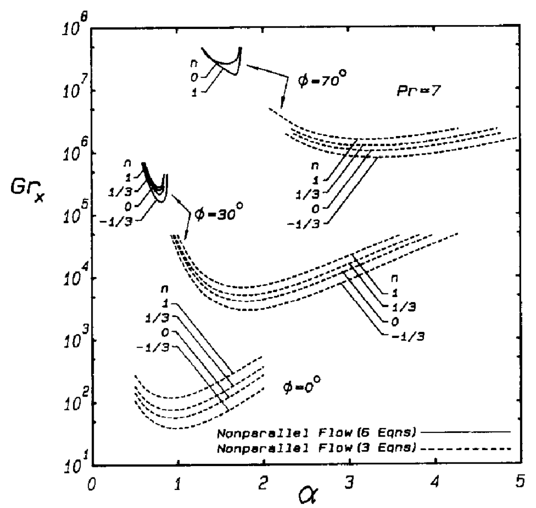

FIG. 6. The effect of n on the neutral stability curves, $Pr = 7$.

7, respectively, for the $n = 0$ (UWT) case. Included in the figures for comparison are results from the parallel flow model reported in ref. [10]. It can be seen from these figures that the critical Grashof numbers from the three-equation non-parallel flow model are about one order of magnitude larger than those from the parallel flow model [10]. The critical Grashof numbers from the six-equation non-parallel flow model are still much larger than those of the three-equation model, about one and two orders of magnitude larger for $Pr = 0.7$ and 7, respectively. From the comparison among these three sets of results, it can be concluded that the more rigorous non-parallel flow analysis, which takes into account the streamwise dependence of the disturbances, predicts critical Grashof numbers that are larger than those predicted by the parallel flow analysis.

It is interesting to compare the vortex instability results from the present analysis based on the six-

Table 2. Critical values of non-similar parameter, Grashof number, and wave number; six-equation local non-similarity non-parallel flow model; $Pr = 0.7$

ϕ (deg)	ξ^*	$n = -1/3$ Gr_x^*	α^*	ξ^*	$n = 0$ (UWT) Gr_x^*	α^*	ξ^*	$n = 1/3$ Gr_x^*	α^*	ξ^*	$n = 1$ Gr_x^*	α^*
0	0	771.9	0.72046	0	834.5	0.68803	0	934.0	0.66405	0	1165	0.62066
15	1.3297	15 579	0.48217	1.32798	15 478	0.44852	1.3199	15 013	0.43023	1.3002	13 926	0.41128
20	2.0072	27 140	0.54939	1.90850	21 092	0.50755	1.8957	20 394	0.48426	1.8642	18 755	0.45882
30	3.6806	60 790	0.65620	3.64009	57 518	0.60275	3.5775	52 740	0.57303	3.4670	45 083	0.53779
45	8.7680	366 430	0.80402	8.54266	321 700	0.73903	8.3069	279 690	0.70578	7.9346	222 390	0.65768
60	21.188	2 739 350	1.0014	20.5638	2 358 900	0.93489	19.928	2 016 120	0.85881	18.719	1 474 400	0.80404
70	44.726	16 712 800	1.1958	43.1669	13 996 000	1.1286	41.557	11 573 600	1.0427	39.198	8 641 060	0.97396

Table 3. Critical values of non-similar parameter, Grashof number, and wave number; six-equation local non-similarity non-parallel flow model; $Pr = 7$

ϕ (deg)	ξ^*	$n = -1/3$ Gr_x^*	α^*	ξ^*	$n = 0$ (UWT) Gr_x^*	α^*	ξ^*	$n = 1/3$ Gr_x^*	α^*	ξ^*	$n = 1$ Gr_x^*	α^*
0	0	37.95	0.98318	0	56.33	0.94275	0	75.26	0.92484	0	117.7	0.90566
10	0.70693	5259	0.52489	0.77364	8255	0.51072	0.81249	10 547	0.50686	0.85909	13 939	0.50651
15	1.3200	15 019	0.60652	1.43432	22 751	0.58986	1.5041	28 848	0.58421	1.5511	33 648	0.58341
30	4.4687	160 379	0.81386	4.73181	213 490	0.79437	4.8641	244 520	0.78875	4.9611	270 480	0.78854
45	10.548	923 285	1.0224	11.0127	1 145 400	1.0024	11.180	1 234 800	0.99748	11.223	1 259 010	0.99986
60	24.257	5 387 440	1.2909	24.9484	6 200 300	1.2583	25.038	6 312 000	1.2545	24.689	5 884 570	1.2545
70	47.911	23 573 500	1.5873	48.9086	26 132 000	1.5811	47.830	23 355 000	1.5816	44.521	16 333 200	1.6996

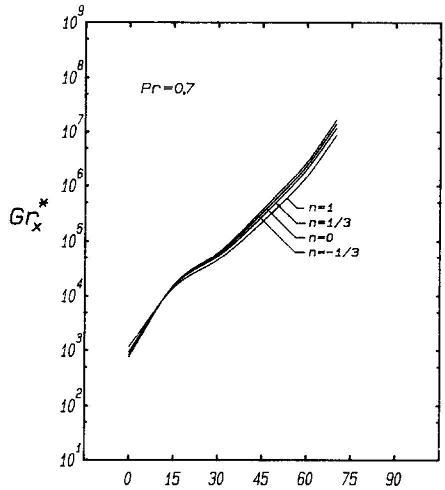

FIG. 7. The effect of n on the critical Grashof numbers, $Pr = 0.7$.

equation non-parallel flow model with previous results from the parallel flow analyses and with available experimental data in the literature [2, 7, 8, 10, 11, 14, 23]. Such a comparison is made in Fig. 11 for $n = 0$ (UWT) and in Fig. 12 for $n = 1/3$ ($\simeq$ UHF). From these two figures it can be seen that the critical Grashof numbers predicted by the six-equation non-parallel flow model are about two orders of magnitude larger than those from the parallel flow analysis, and are in qualitative agreement with available experimental values for air ($Pr = 0.7$) and water ($Pr = 7$), particularly for the latter.

It is noted here that both the parallel flow model and the three-equation non-parallel flow model predict, for all angles of inclination, critical Grashof

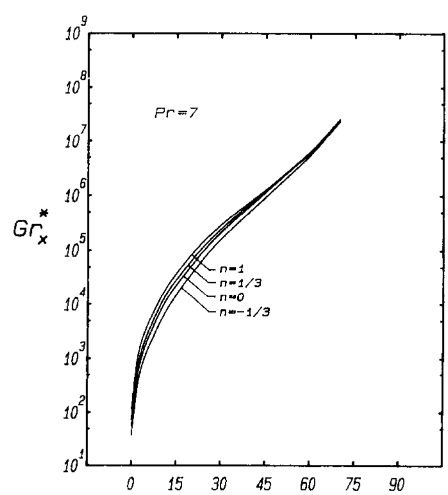

FIG. 8. The effect of n on the critical Grashof numbers, $Pr = 7$.

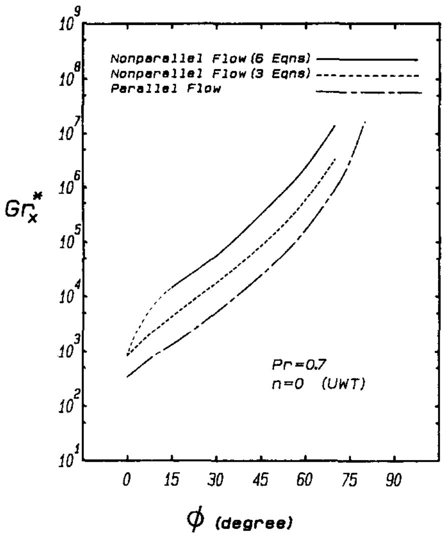

FIG. 9. A comparison of the critical Grashof numbers between the non-parallel flow model and the parallel flow model, uniform wall temperature (UWT, $n = 0$), $Pr = 0.7$.

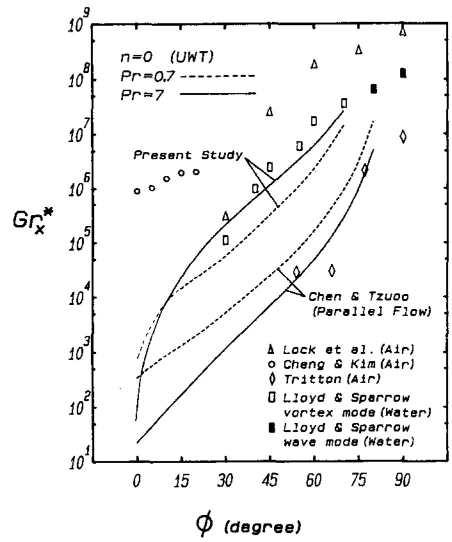

FIG. 11. A comparison of the critical Grashof numbers between analyses and experimental data, uniform wall temperature (UWT, $n = 0$).

numbers, Gr_x^*, that are larger for $Pr = 0.7$ than for $Pr = 7$ (see Figs. 11 and 12, and compare Figs. 9 and 10). On the other hand, the six-equation non-parallel flow model yields smaller Gr_x^* values for $Pr = 0.7$ as compared to $Pr = 7$ for most of the inclination angles from the horizontal that are not very small (i.e. $\phi > 8°$ for the case of $n = 0$ and $\phi > 5°$ for the case of $n = 1/3$). The reason for such a change in the ordering of the Gr_x^* vs ϕ curves among the various models for the two Prandtl numbers is not clear and cannot be explained. A thorough checking has concluded that it is not due to numerical errors. In addition, it should be mentioned that the critical Grashof numbers for very small angles of inclination (i.e. $\phi \simeq 0°$) are not expected to be very accurate, because the mainflow solution based on the boundary-layer assumption does not have good approximations when $Gr_x < 10^3$.

Because no experimental studies on vortex instability of natural convection flow on inclined flat plates are available under the power-law wall temperature variation except for the UWT case ($n = 0$) and UHF case ($n \simeq 1/3$), the present results from the non-parallel analysis, other than the cases of $n = 0$ and $1/3$, cannot be verified directly with experimental data.

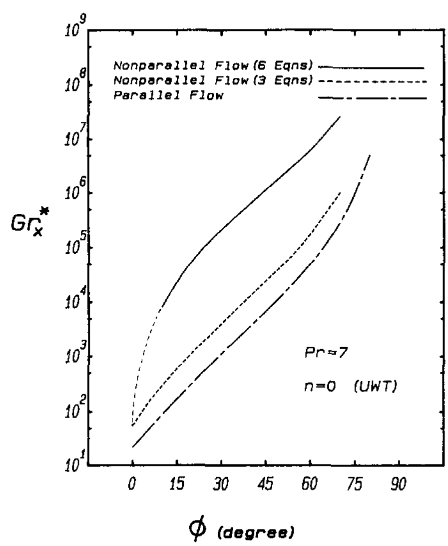

FIG. 10. A comparison of the critical Grashof numbers between the non-parallel flow model and the parallel flow model, uniform wall temperature (UWT, $n = 0$), $Pr = 7$.

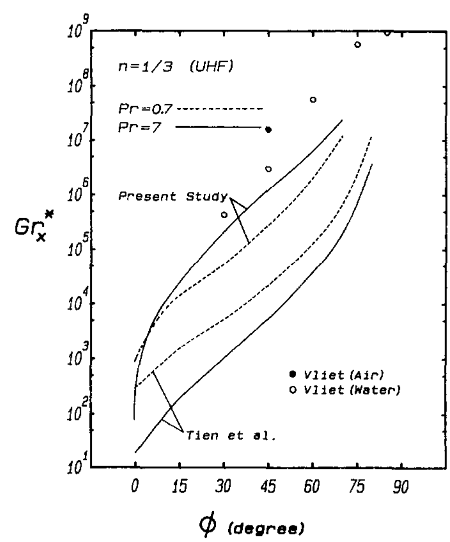

FIG. 12. A comparison of the critical Grashof numbers between analyses and experimental data, uniform surface heat flux (UHF, $n \simeq 1/3$).

CONCLUSION

In this paper, vortex instability of laminar boundary-layer flow in natural convection on inclined flat plates with a power-law variation in wall temperature has been investigated analytically by employing the linear non-parallel flow theory. Neutral stability curves, critical Grashof numbers, and critical wave numbers are presented for fluids having $Pr = 0.7$ and 7 over a wide range of inclination angles from the horizontal, $0^\circ \leqslant \phi \leqslant 70^\circ$, for a range of exponent values n from $-1/3$ to 1. In general, it is found that the flow becomes more stable to the vortex mode of instability as the inclination angle from the horizontal increases. The more rigorous non-parallel flow model, which takes into account the streamwise dependence of the disturbances, predicts critical Grashof numbers that are larger than those predicted by the parallel flow model. In addition, the six-equation non-parallel flow model has yielded critical Grashof numbers that are in close and qualitative agreement with available experimental data for the cases of heating by uniform wall temperature (UWT, $n = 0$) and uniform surface heat flux (UHF, $n \simeq 1/3$).

It is also found that for a given value of the exponent n, the critical Grashof number increases with increasing Prandtl number for larger inclination angles. However, this trend is reversed for smaller angles of inclination. For $Pr = 7$, at a given inclination angle $\phi < 60^\circ$ the critical Grashof number increases with increasing value of the exponent n. However, for $Pr = 0.7$ the critical Grashof number decreases with increasing value of the exponent n at larger inclination angles, but this trend is reversed for small angles of inclination ($\phi \simeq 0$).

Acknowledgement—Part of the numerical results reported in this paper was obtained by using a CRAY X-MP Supercomputer through the facility of National Center for Supercomputing Applications (NCSA) at the University of Illinois.

REFERENCES

1. E. M. Sparrow and R. B. Husar, Longitudinal vortices in natural convection flow on inclined surfaces, *J. Fluid Mech.* **37**, 251–255 (1969).
2. J. R. Lloyd and E. M. Sparrow, On the instability of natural convection flow on inclined plates, *J. Fluid Mech.* **42**, 465–470 (1970).
3. G. J. Hwang and K. C. Cheng, Thermal instability of laminar natural convection flow on inclined isothermal plates, *Can. J. Chem. Engng* **51**, 659–666 (1973).
4. S. E. Haaland and E. M. Sparrow, Vortex instability of natural convection flow on inclined surfaces, *Int. J. Heat Mass Transfer* **16**, 2355–2367 (1973).
5. R. A. Kahawita and R. N. Meroney, The vortex mode of instability in natural convection flow along inclined plates, *Int. J. Heat Mass Transfer* **17**, 541–548 (1974).
6. P. A. Iyer and R. E. Kelly, The instability of the laminar free convection flow induced by a heated inclined plate, *Int. J. Heat Mass Transfer* **17**, 517–525 (1974).
7. G. S. H. Lock, C. Gort and G. R. Pond, A study of instability in free convection from an inclined plate, *Appl. Scient. Res.* **18**, 171–182 (1967).
8. D. J. Tritton, Transition to turbulence in the free convection boundary layers on an inclined heat plate, *J. Fluid Mech.* **16**, 417–435 (1963).
9. J. R. Lloyd, Vortex wavelength in the transition flow adjacent to upward facing inclined isothermal surfaces, *Proc. 5th Int. Heat Transfer Conf.*, Vol. III, Paper No. NC1.8, pp. 34–37 (1974).
10. T. S. Chen and K. L. Tzuoo, Vortex instability of free convection flow over horizontal and inclined surfaces, *J. Heat Transfer* **104**, 637–643 (1982).
11. H. C. Tien, T. S. Chen and B. F. Armaly, Vortex instability of natural convection flow over horizontal and inclined plates with uniform surface heat flux, *Numer. Heat Transfer* **9**, 697–713 (1986).
12. C. T. Hsu, P. Cheng and G. M. Homsy, Instability of free convection flow over a horizontal impermeable surface in a porous medium, *Int. J. Heat Mass Transfer* **21**, 1221–1228 (1978).
13. C. T. Hsu and P. Cheng, Vortex instability in buoyancy-induced flow over inclined heated surfaces in porous media, *J. Heat Transfer* **101**, 660–665 (1979).
14. K. C. Cheng and Y. W. Kim, Flow visualization studies on vortex instability of natural convection flow over horizontal and slightly inclined constant-temperature plates, *J. Heat Transfer* **110**, 608–615 (1988).
15. H. R. Lee, T. S. Chen and B. F. Armaly, Non-parallel vortex instability of natural convection flow over a non-isothermal horizontal flat plate, *Int. J. Heat Mass Transfer* **34**, 305–313 (1991).
16. K. Chen and M. M. Chen, Thermal instability of forced convection boundary layers, *J. Heat Transfer* **106**, 284–289 (1984).
17. J. Y. Yoo, P. Park, C. K. Choi and S. T. Ro, An analysis on the thermal instability of forced convection flow over isothermal horizontal flat plate, *Int. J. Heat Mass Transfer* **30**, 927–935 (1987).
18. H. R. Lee, T. S. Chen and B. F. Armaly, Non-parallel thermal instability of forced convection flow over a heated, non-isothermal horizontal flat plate, *Int. J. Heat Mass Transfer* **33**, 2019–2028 (1990).
19. S. L. Lee, T. S. Chen and B. F. Armaly, New finite difference solution methods for wave instability problems, *Numer. Heat Transfer* **10**, 1–18 (1986).
20. T. S. Chen, H. C. Tien and B. F. Armaly, Natural convection on horizontal, inclined, and vertical plates with variable surface temperature or heat flux, *Int. J. Heat Mass Transfer* **29**, 1465–1478 (1986).
21. E. M. Sparrow, H. Quack and C. J. Boerner, Local nonsimilarity boundary-layer solutions, *AIAA J.* **8**(11), 1936–1942 (1970).
22. E. M. Sparrow and H. S. Yu, Local nonsimilarity thermal boundary-layer solutions, *J. Heat Transfer* **93**, 328–334 (1971).
23. G. C. Vliet, Natural convection local heat transfer on constant-heat-flux inclined surfaces, *J. Heat Transfer* **91**, 511–516 (1969).

APPENDIX

The coefficients in equations (44)–(49) are given by

$$a_1 = -C_1,\quad a_2 = C_2-\alpha^2,\quad a_3 = -5f''(Gr_x\cos\phi/5)^{1/5},$$
$$a_4 = 5\xi,\quad a_5 = -3\xi f',$$
$$b_1 = -C_1,\quad b_2 = C_4-2\alpha^2,$$
$$b_3 = 2f''+\alpha^2C_1,\quad b_4 = \alpha^4+\alpha^2C_2,$$
$$b_5 = -(\alpha^2/5)(Gr_x\cos\phi/5)^{-1/5}C_3,$$
$$b_6 = -5\alpha^2(Gr_x\cos\phi/5)^{1/5},$$
$$b_7 = -3\xi f',\quad b_8 = -3\xi f'',\quad b_9 = 3\alpha^2\xi f',$$
$$d_1 = -Pr\,C_1,\quad d_2 = Pr\,f'-\alpha^2,\quad d_3 = -(Pr/5)C_5,$$
$$d_4 = -Pr\,\theta'(Gr_x\cos\phi/5)^{1/5},\quad d_5 = -3Pr\,\xi f',$$

$$e_1 = -C_1,\quad e_2 = C_2 - C_4 + 2f' - \alpha^2,$$
$$e_3 = -5f''(Gr_x\cos\phi/5)^{1/5},\quad e_4 = 5\xi,\quad e_5 = C_6,\quad e_6 = C_7,$$
$$e_7 = -5(Gr_x\cos\phi/5)^{1/5}(C_9 + f''/\xi),\quad e_8 = 5,$$
$$f_1 = -C_1,\quad f_2 = 2f' - 2\alpha^2,\quad f_3 = C_1\alpha^2 - f'' - 3\xi C_9,$$
$$f_4 = \alpha^4 + \alpha^2(C_2 + C_4 - 2f'),\quad f_5 = b_5,\quad f_6 = b_6,$$
$$f_7 = C_6,\quad f_8 = C_{10},\quad f_9 = 2C_9 - \alpha^2 C_6,$$
$$f_{10} = \alpha^2 C_7,\quad f_{11} = (\alpha^2/5)(Gr_x\cos\phi/5)^{-1/5}[(C_3/\xi) - C_8],$$
$$f_{12} = -(5\alpha^2/\xi)(Gr_x\cos\phi/5)^{1/5},$$
$$g_1 = -Pr\,C_1,\quad g_2 = -\alpha^2 - Pr(C_4 - 3f'),$$
$$g_3 = -(Pr/5)C_5,\quad g_4 = -Pr\,\theta'(Gr_x\cos\phi/5)^{1/5},$$
$$g_5 = Pr\,C_6,\quad g_6 = Pr\,C_{13},\quad g_7 = -(Pr/5)C_{11},$$
$$g_8 = -(Pr/\xi)(Gr_x\cos\phi/5)^{1/5}C_{12} \qquad \text{(A1)}$$

where $C_1(\xi,\eta)$ through $C_{13}(\xi,\eta)$ are given by

$$C_1(\xi,\eta) = -3(f + \xi\,\partial f/\partial\xi),$$
$$C_2(\xi,\eta) = 2\eta f'' - f' - 3\xi\,\partial f'/\partial\xi,$$
$$C_3(\xi,\eta) = 4\eta^2 f'' + 2\eta f' - 6f - 12\eta\xi\,\partial f'/\partial\xi + 12\xi\,\partial f/\partial\xi + 9\xi^2\,\partial^2 f\,\partial\xi^2,$$
$$C_4(\xi,\eta) = 5f' + 3\xi\,\partial f'/\partial\xi,\quad C_5(\xi,\eta) = 3\xi\,\partial\theta/\partial\xi - 2\eta\theta',$$
$$C_6(\xi,\eta) = 6\,\partial f/\partial\xi + 3\xi\,\partial^2 f/\partial\xi^2,$$
$$C_7(\xi,\eta) = 2\eta\,\partial f''/\partial\xi - 4\,\partial f'/\partial\xi - 3\xi\,\partial^2 f'/\partial\xi^2,$$
$$C_8(\xi,\eta) = 4\eta^2\,\partial f''/\partial\xi - 10\eta\,\partial f'/\partial\xi + 6\,\partial f/\partial\xi + 30\xi\,\partial^2 f/\partial\xi^2 - 12\eta\xi\,\partial^2 f'/\partial\xi^2 + 9\xi^2\,\partial^3 f/\partial\xi^3,$$
$$C_9(\xi,\eta) = \partial f''/\partial\xi,\quad C_{10}(\xi,\eta) = 8\,\partial f'/\partial\xi + 3\xi\,\partial^2 f'/\partial\xi^2,$$
$$C_{11}(\xi,\eta) = 3\,\partial\theta/\partial\xi - 2\eta\,\partial\theta'/\partial\xi + 3\xi\,\partial^2\theta/\partial\xi^2,$$
$$C_{12}(\xi,\eta) = \theta' + \xi\,\partial\theta'/\partial\xi,\quad C_{13}(\xi,\eta) = \partial f'/\partial\xi. \qquad \text{(A2)}$$

INSTABILITE THERMIQUE NON PARALLELE DE LA CONVECTION SUR DES PLAQUES PLANES INCLINEES ET NON ISOTHERMES

Résumé—On étudie analytiquement en théorie linéaire, les caractéristiques de l'instabilité tourbillonnaire de l'écoulement laminaire de couche limite, dans la convection naturelle sur des plaques planes inclinées, chauffées par dessous, avec une température de surface variable comme $T_w(x) - T_\infty = Ax^n$. L'écoulement principal est bidimensionnel et on prend en compte la dépendance dans la direction de l'ecoulement des fonctions amplitude de perturbation. On présente les courbes de stabilité neutre, les nombres de GRASHOF critiques et les nombres d'onde critiques correspondants pour des fluides ayant $Pr = 0{,}7$ et 7, pour des angles d'inclinaison $0° \leqslant \phi \leqslant 70°$ à partir de l'horizontale, pour un exposant n entre $-1/3$ et 1. Pour un nombre de PRANDTL et n donnés, l'écoulement est plus stable, vis-à-vis de l'instabilité tourbillonnaire, quand l'angle d'inclinaison augmente. La dépendance des perturbations dans le sens de l'écoulement conduit à une stabilisation de l'écoulement principal ce qui fait que les prédictions s'accordent qualitativement avec les données expérimentales.

NICHTPARALLELE THERMISCHE INSTABILITÄT BEI NATÜRLICHER KONVEKTION AN NICHTISOTHERMEN GENEIGTEN EBENEN FLÄCHEN

Zusammenfassung—Das Verhalten laminarer Grenzschichtströmungen im Hinblick auf Wirbelinstabilität bei natürlicher Konvektion an einer von unten beheizten geneigten ebenen Platte mit veränderlicher Oberflächentemperatur ($T_w(x) - T_\infty = Ax^n$) wird analytisch mit der Theorie linearer Lösungen untersucht. Dabei wird ein Modell für nichtparallele Strömung angewandt, bei dem die stationäre Hauptströmung zweidimensional behandelt wird und Veränderungen der Störungsamplitude in Strömungsrichtung berücksichtigt werden. Die Kurven neutraler Stabilität wie auch die kritische Grashof-Zahl und die entsprechende kritische Wellenzahl werden für folgende Bedingungen dargestellt: Prandtl-Zahl des Fluids ($Pr = 0{,}7$ und 7); Neigungswinkel ($0° \leqslant \phi \leqslant 70°$ gegenüber der Waagerechten); Exponenten n ($-1/3 < n < 1$). Es zeigt sich, daß bei gegebenen Werten der Prandtl-Zahl und des Exponenten n die Strömung im Hinblick auf die Wirbelinstabilität stabiler wird, wenn der Neigungswinkel von der Horizontalen zunimmt. Weiterhin ergibt das nichtparallele Strömungsmodell mit lokaler Nichtähnlichkeit eine größere kritische Grashof-Zahl als das Modell mit lokaler Ähnlichkeit. Die Ergebnisse der vorgestellten Untersuchung für nichtparallele Strömung werden mit den entsprechenden Ergebnissen früherer Untersuchungen an paralleler Strömung und mit verfügbaren Versuchsdaten vergleichen. Die Veränderung der Störungen in Strömungsrichtung führt zu einer Stabilisierung der Hauptströmung. Dies führt dann dazu, daß die vorgestellten Rechenergebnisse qualitativ gut mit verfügbaren Versuchsdaten übereinstimmen.

НЕПАРАЛЛЕЛЬНАЯ ТЕПЛОВАЯ НЕУСТОЙЧИВОСТЬ ЕСТЕСТВЕННОКОНВЕКТИВНОГО ТЕЧЕНИЯ НА НЕИЗОТЕРМИЧЕСКИХ НАКЛОННЫХ ПЛОСКИХ ПЛАСТИНАХ

Аннотация—На основе линейной теории анализируются характеристики вихревой неустойчивости ламинарного течения в пограничном слое в условиях естественной конвекции на нагреваемых снизу наклонных плоских пластинах при переменной температуре поверхности $T_w(x) - T_\infty = Ax^n$. Анализ проводится с использованием модели непараллельного течения, в которой устойчивое основное течение рассматривается как двумерное и учитывается зависимость функций амплитуды возмущения от расстояния вниз по потоку. Представлены кривые нейтрального равновесия, а также критические числа Грасгофа и соответствующие критические волновые числа для жидкостей с $Pr = 0{,}7$ и 7 в диапазоне изменения угла наклона $0° \leqslant \phi \leqslant 70°$ относительно горизонтали в интервале изменения показания степени n от $-1/3$ до 1. При данных значениях числа Прандтля и показателе степени n найдено, что течение приближается к вихревому режиму неустойчивости по мере увеличения угла наклона относительно горизонтали. Кроме того, при использовании модели локальной неавтомодельности непараллельного течения получается более высокое значение критического числа Грасгофа, чем в модели локальной автомодельности непараллельного течения. Результаты анализа непараллельных течений сравниваются с данными, полученными ранее на основе анализа параллельных течений, и с имеющимися экспериментальными результатами. Зависимость возмущений от расстояния вниз по потоку приводит к стабилизации основного потока, благодаря чему наблюдается качественное согласие между теоретическими результатами и имеющимися экспериментальными данными.